Journal of Catalysis 405 (2022) 288–302

Contents lists available at ScienceDirect

Journal of Catalysis

journal homepage: www.elsevier.com/locate/jcat

Synthesis of Florol via Prins cyclization over heterogeneous catalysts

Basile Lasne [a], Päivi Mäki-Arvela [a], Atte Aho [a], Zuzana Vajglova [a], Kari Eränen [a], Narendra Kumar [a], Julián E. Sánchez-Velandia [b], Markus Peurla [c], Cecilia Mondelli [d], Javier Pérez-Ramírez [d], Dmitry Yu Murzin [a,*]

[a] Laboratory of Industrial Chemistry and Reaction Engineering, Åbo Akademi University, Henriksgatan 2, 20500 Turku/Åbo, Finland
[b] Grupo de Investigación Fitoquímica Universidad Javeriana, Pontificia Universidad Javeriana, Bogotá, Colombia
[c] Faculty of Medicine, University of Turku, 20500 Turku/Åbo, Finland
[d] Institute of Chemical and Bioengineering, Department of Chemistry and Applied Biosciences, ETH Zürich, Vladimir-Prelog-Weg 1, 8093 Zürich, Switzerland

ARTICLE INFO

Article history:
Received 10 November 2021
Revised 9 December 2021
Accepted 11 December 2021
Available online 17 December 2021

Keywords:
Florol
Prins cyclization
Isoprenol
Isovaleraldehyde
Zeolites
Mesoporous materials
DFT

ABSTRACT

In this work, several heterogeneous micro- and mesoporous, acidic catalysts were tested for the selective synthesis of Florol®, an industrial product formed via condensation and rehydration starting from isoprenol and isovaleraldehyde in dimethylcarbonate as a solvent. The results showed that a mildly acidic, microporous H-Beta-300 with SiO_2/Al_2O_3 ratio of 300 was the best catalyst, giving 72% selectivity with 99% conversion at 40 °C when using the molar ratio isoprenol to isovaleraldehyde of 1:5. More acidic zeolites gave slightly lower selectivity, while the lowest selectivity (up to 52%) was obtained with mesoporous catalysts exhibiting mild acidity and no strong Brønsted acid sites. Selectivity to pyranols was nearly constant when changing temperature, while a larger excess of isovaleraldehyde promoted formation of tetrahydropyranol. H-Beta-300 catalyst was successfully after calcination at 400 °C. DFT calculations pointed out on the parallel formation of tetrahydro pyranols and dihydropyrans, which are the corresponding dehydration products.

1. Introduction

Synthesis of fine chemicals, e.g., pharmaceuticals and perfumes from biomass derived feedstock has been recently a highly interesting research topic. Furthermore, heterogeneous catalysts, which are relatively inexpensive and easy to recover and recycle, have been extensively used in the field. There are, however still some reactions, which have been scarcely studied, such as the Prins cyclization of a homoallylic alcohol with an aldehyde [1–3], for example isoprenol with isovaleraldehyde to produce Florol®, a commercial product, finding application in the fragrance industry [1,4–10]. The starting materials are obtained from biomass, e.g., isovaleraldehyde from pyrolysis of microalga [11] and isoprenol via fermentation of glucose [12].

Prins cyclization of isoprenol with isovaleraldehyde produces both cis and trans isomers, out of which the former one is the desired product [13]. In addition to these, also three dehydration products can be obtained (Fig. 1) either in a consecutive or parallel pathways.

There are few studies in the literature reporting synthesis of different tetrahydropyran like compounds. For example, the highest yield of the desired tetrahydropyranol was 54% when using a homogeneous iron nitrate catalyst in Prins cyclization of isoprenol with isovaleraldehyde (1:1 M ratio, water as a solvent, 90 °C and 5 h) [6]. On the other hand, only 14% yield of the desired target was obtained under similar conditions over Fe-modified silica gel. A heterogeneous ion-exchange resin, Amberlyst 15 was a rather efficient catalyst for this reaction, giving 68% of selectivity and a high ratio between the desired and dehydration products in the presence of water at 70 °C. The authors did not report, however, the conversion level [4]. The same catalyst gave 51% yield of tetrahydropyranol after 11 h at 70–80 °C in the absence of any solvent [1]. In addition, in a patent, the yield of pyranols was *ca.* 76% over a strongly acidic cationic exchanger resin, Amberlyst 131, with a small excess of isoprenol, at unspecified temperature somewhere between 0 and 70 °C [8]. Analogously, in [14] Amberlyst 131 gave a 73% yield of tetrahydropyranol after 10 h at 25 °C in the presence of water. In addition, 49% yield of THP was obtained over MoO_3/SiO_2 when using isovaleraldehyde to isoprenol ratio of 0.9:1 after 5 h [5]. Phosphotungstic and molybdic acids either as homogeneous catalysts or immobilized on MCM-41 were also used in this reaction [4] giving the best selectivity of 96% at 80 °C when

* Corresponding author.
E-mail address: dmitry.murzin@abo.fi (D.Y. Murzin).

https://doi.org/10.1016/j.jcat.2021.12.008
0021-9517/

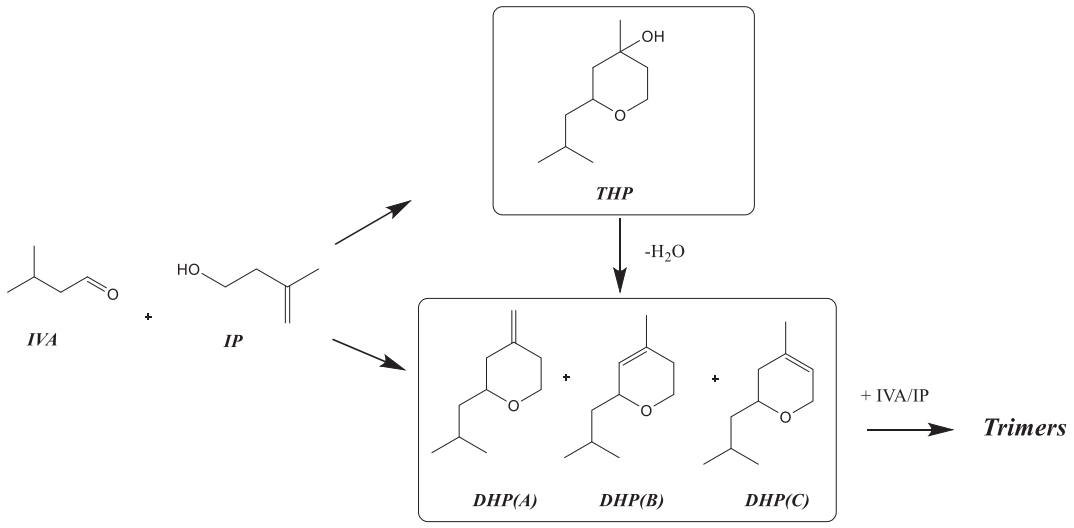

Fig. 1. Reaction scheme for the synthesis of tetrahydropyranol (THP) from isovaleraldehyde (IVA) and isoprenol (IP). The undesired dehydration products are denoted as DHP (A), DHP(B), DHP(C) and after addition of either IVA or IP molecule to these, forming trimeric compounds.

isovaleraldehyde conversion was 70% at 3 h reaction time. Analogously $Cs_{2.5}H_{0.5}PW_{12}O_{40}$ supported on silica was a very efficient catalyst in the studied reaction when 10:1 M ratio of isovaleraldehyde to isoprenol was used at 30 °C in dimethylcarbonate and a small amount of water was added as a solvent giving complete conversion of isoprenol and 80% yield of tetrahydropyranol in 1 h [9]. The *K*10 (commercial montmorillonite) clay gave maximally 72% of yield of the desired tetrahydropyranols at 40 °C [7].

The kinetics of tetrahydropyranol formation has been scarcely studied, apart from few reports addressing for example, selectivity to tetrahydropyranols as a function of conversion [7]. Otherwise, typically kinetic analysis is very limited or even absent [1,4,5]. In [5] the rate constants for this reaction were calculated, without presenting the kinetic profiles. In [9], the Prins cyclization of isoprenol with isovaleraldehyde was investigated over mesoporous phosphotungstic acid catalysts optimizing such reaction conditions, as time, molar ratio of the reactants, and temperature. However, no kinetic profiles or activation energy were reported. Furthermore, and as can be seen from the overview above, the range of catalytic materials reported in the literature is very limited, not covering in particular various micro- and mesoporous catalysts with different size of the pores, morphology and acidity. Considering all these aspects, the aim of this work was to investigate kinetics of the Prins cyclization of isoprenol with isovaleraldehyde over different micro- and mesoporous catalysts. Subsequently, the main focus of the current work was to study physico-chemical properties of the catalysts, such as morphology, shape, size as well as acidity. For the best performing catalysts, the effect of the reaction temperature, the feed ratio of reactants as well as the catalyst recycling were investigated. In all cases the detailed concentration profiles are reported.

2. Experimental

2.1. Materials

Isoprenol and isovaleraldehyde (97% purity) as well as dimethyl carbonate (99% purity) were purchased from Sigma-Aldrich and used as received without additional purification or drying. Argon 5.0 (99.999%) was from AGA. Iron(III) acetate was purchased from Riedel-de Haën. This study was first focused on microporous H-Beta-38, -150, -300 (Zeolyst International, the number denotes SiO_2/Al_2O_3 ratio), and on H-USY-30 (Zeolyst International, CBV760, Si/Al = 30, proton form).

2.2. Catalyst preparation

H-USY-30 was modified by an alkaline treatment in an aqueous NaOH solution (0.3 M, 30 mL per gram of dried zeolite) containing 0.2 M of TPABr (ABCR, 98%) at 65 °C for 30 min in an Easymax 102 reactor (Mettler Toledo). The resulting material was converted into the protonic form by three consecutive ion exchange steps in an aqueous NH_4NO_3 solution (0.1 M, 25 °C, 6 h, 100 mL per gram of zeolite), subsequent thermal treatment in static air at 550 °C (5 °C min^{-1}) for 5 h. This modified sample was denoted by the code AT.

The details of the preparation of micro-mesoporous composite materials comprising MCM-41 and a Beta zeolite, denoted as H-NK-MM-BE-B, H-NK-MM-BE-C are given in [15]. H-MCM-41-F was prepared according to the recipe given in [16].

Fe-H-Beta-38 was synthesized using the ion-exchange method. Iron (III) acetate (3.58 g) was dissolved in 500 mL of distilled water and the pH was measured giving the value of 2.19. Then, the solution was stirred under mechanical stirring (160 rpm) and the H-Beta-38 zeolite (10 g) was slowly added to the mixture. The pH was measured again giving the value of 2.16, and the solution was left under stirring for 24 h. Afterwards, the solution was filtered and the recovered solid was washed with 2 L of distilled water and dried in an oven at 100 °C for at least 7 h. The catalyst was weighed and calcined to decompose Fe acetate precursor. The calcination was performed using a step calcination procedure: 75 min–250 °C, 50 min–250 °C, 60 min–450 °C, 180 min–450 °C, 100 min–25 °C. The above procedure was repeated using H-Beta-300 to make the Fe-H-Beta-300 catalyst.

2.3. Catalyst characterization

Some catalysts have been characterized previously, while for those not yet reported in the literature the catalyst texture and acidity were investigated. Nitrogen physisorption (Micromeritics 3Flex) was used to measure the surface areas, pore sizes and volumes. The samples were outgassed at 180 °C for 24 h prior to measurements. The Brunauer-Emmett-Teller (BET) method was used

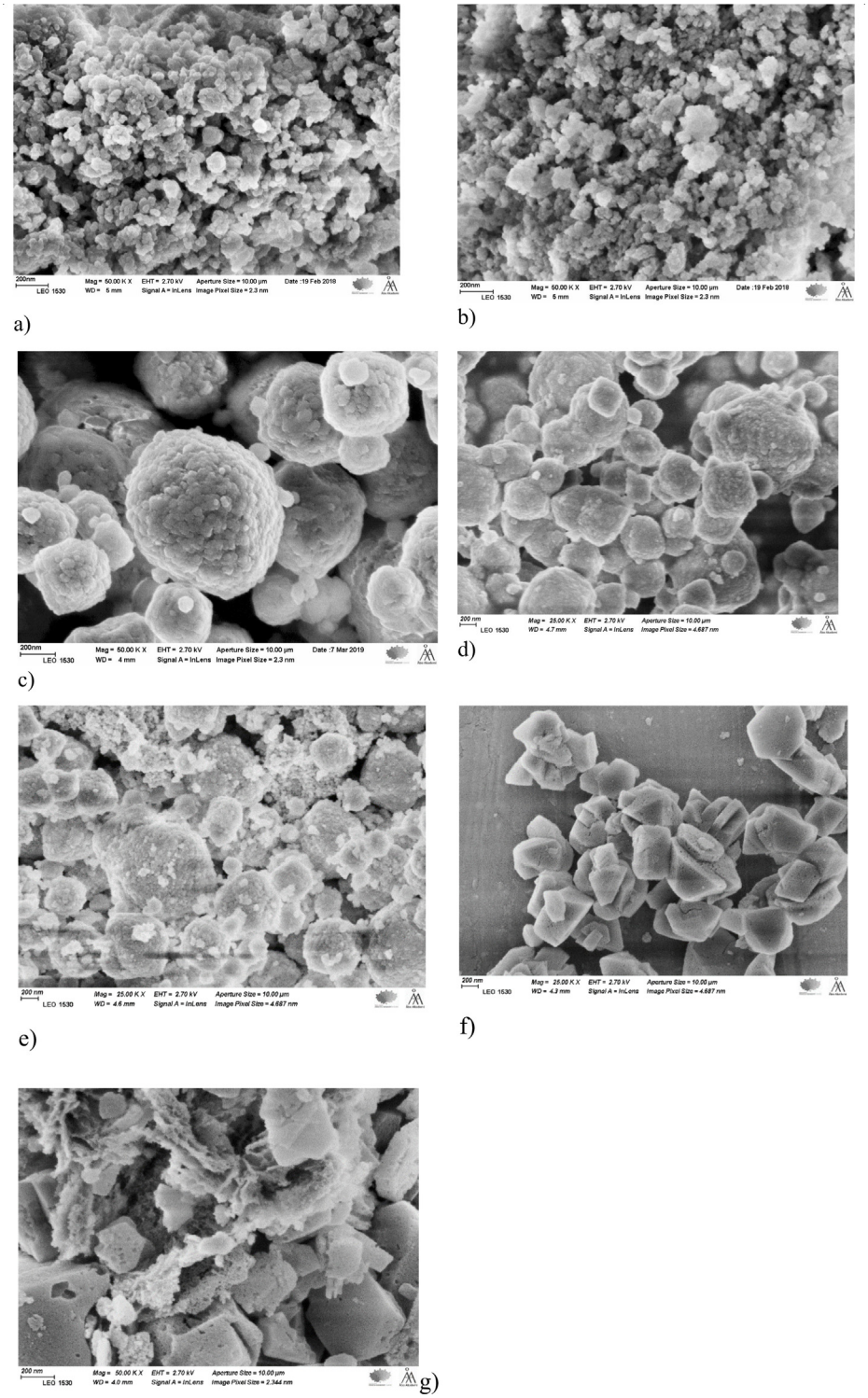

Fig. 2. SEM images a) H-Beta-300, b) H-Beta-150, c) H-Beta-38, d) Fe-H-Beta-300, e) Fe-H-Beta-38, f) H-USY-30 and g) H-USY-30-AT.

for determination of the specific surface areas for both microporous and mesoporous materials.

Catalyst morphology was investigated using transmission electron microscopy. A JEOL 2010 microscope was used. In addition, the crystal morphology of the catalysts was studied by scanning electron microscopy (SEM) using a Zeiss Leo Gemini 1530 Scanning Electron Microscope with a Thermo Scientific UltraDry Silicon Drift Detector (SDD).

FTIR pyridine adsorption–desorption was performed with ATI Mattson Infinity Series FTIR). The amounts of Brønsted and Lewis acid sites were determined via integrating the peaks corresponding to 1645 cm^{-1} and 1450 cm^{-1} and for quantification the molar extinction factors by [17] were applied. In addition, desorption of pyridine was determined at 250 °C, 350 °C and 450 °C corresponding to the weak, medium and strong acid sites, respectively, as also applied previously [7].

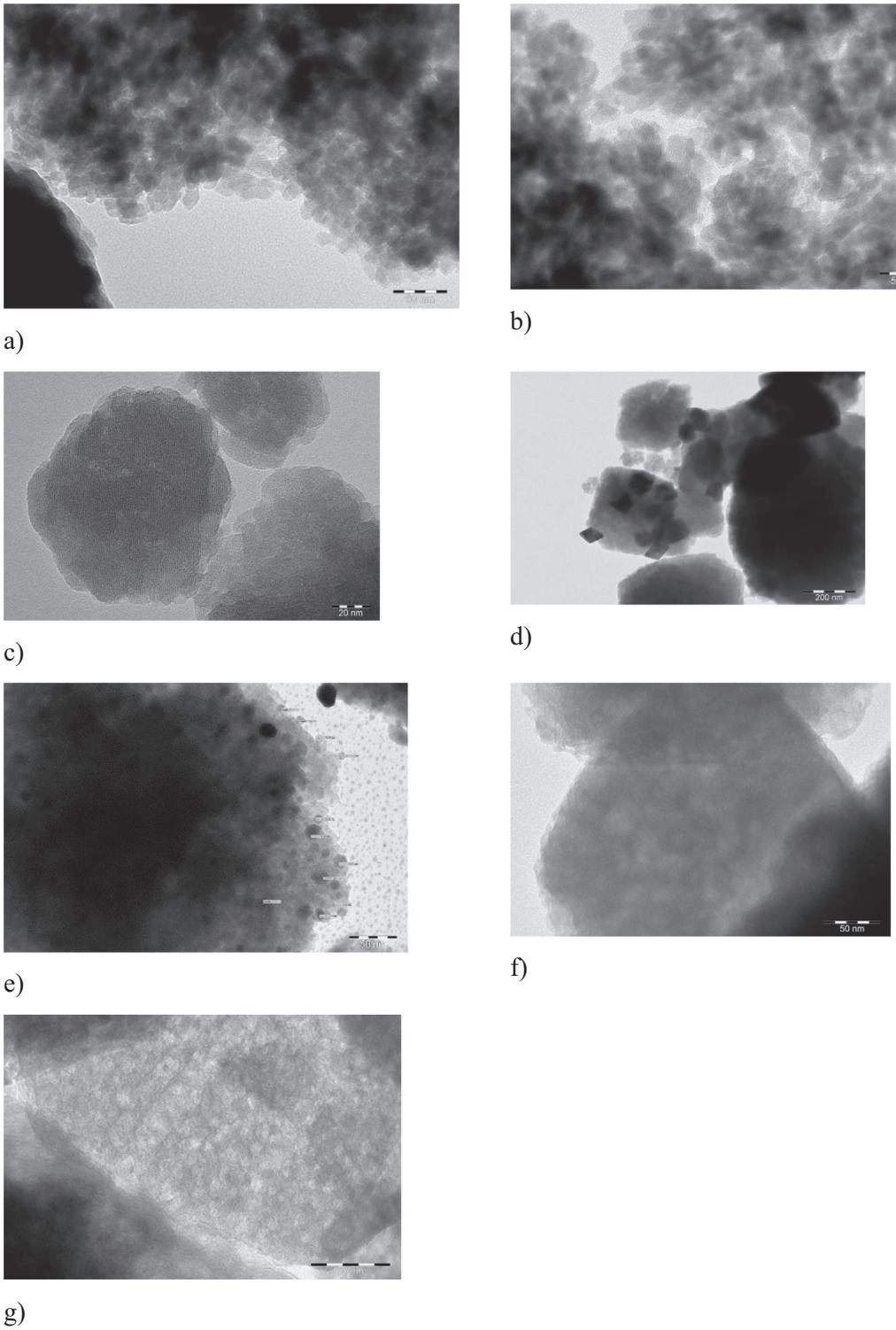

Fig. 3. TEM images of a) H-Beta-300, b) H-Beta-150, c) H-Beta-38, d) Fe-H-Beta-300, e) Fe-H-Beta-38, f) H-USY-30 and g) H-USY-30-AT.

2.4. Catalytic tests

The reaction was carried out in a glass batch reactor mechanically stirred (390 rpm) to exclude external mass transfer limitations. The solvent was pre-heated at 40 °C in an oil bath, in an inert atmosphere composed of argon (2 bar) and cooled by a refrigerant to avoid vaporization of the mixture. The internal temperature was controlled by a thermometer connected to a computer. In a typical experiment, isoprenol (0.860 g, 10 mmol) and isovaleraldehyde (4.300 g, 50 mmol) were added together with dimethyl carbonate to reach a total volume of 50 mL. Then 0.15 g of catalyst, which was sieved to have particles smaller than 71 μm to suppress internal mass transfer limitations and dried overnight at 100 °C, was quickly added and the reaction was initiated by starting the stirring. Samples of around 0.5 mL were taken with a syringe through a septum at different time intervals. After 180 min the

Table 1
Textural properties of the catalysts.

Catalyst	Surface area (m^2/g)	Median pore width (nm)	Specific pore volume (cm^3/g)	V_{meso} (cm^3/g)	V_{micro} (cm^3/g)	V_{meso}/ V_{micro}
H-Beta-300 [21]	629	0.68	0.46	0.24	48	1.09
H-Beta-150 [21]	553		0.63	0.43	32	2.15
H-Beta-38 [22]	827	0.68	n.a.	n.a.	n.a.	n.a.
7.9 wt% Fe-H-Beta-300	461	0.68	0.16	n.a.	n.a.	n.a.
20.3 wt% Fe-H-Beta-38	412	0.68	0.15	n.a.	n.a.	n.a.
H-USY-30 [24]	767	0.77	0.26	n.a.	n.a.	n.a.
H-USY-30-AT	616	0.80	0.21	n.a.	n.a.	n.a.
H-MMBE-B	734	3.08	0.57	0.50	n.a.	n.a.
H-MMBEC	690	3.00	0.51	0.44	n.a.	n.a.
H-MCM-41	885	3.30	0.69	0.55	n.a.	n.a.

Table 2
Results from catalyst acidity measurements through pyridine adsorption–desorption.

Catalyst	Concentration of BA (μmol/g)			Concentration of LA (μmol/g)			Total (μmol/g)	BA/LA ratio	Ref-
	w + m + s	m + s	s	w + m + s	m + s	s			
H-Beta-300	54	49	23	28	9	4	82	1.93	[24]
H-Beta-150	217	178	102	125	63	30	342	1.74	[24]
H-Beta-38	279	261	221	31	12	2	310	8.97	This work
Fe-H-Beta-300	94	44	0	39	8	0	133	2.41	This work
Fe-H-Beta-38	203	142	0	63	9	0	266	3.22	This work
H-USY-30	152	133	25	45	5	1	197	3.38	[23]
H-USY-30-AT	96	44	0	39	8	0	135	2.46	This work
H-MMBE-B	67	31	0	58	11	0	125	1.16	[16]
H-MMBE-C	82	58	0	78	35	0	160	1.05	[16]
H-MCM-41	89	n.d.	n.d.	168	n.d.	n.d.	257	0.53	[25]

Notation: Brønsted acid sites BA, Lewis acid sites LA. [a]w = weak, m = medium, s = strong.

Table 3
Results from the Prins cyclization using different masses of the H-Beta-150 catalyst.

Catalyst mass (g)	$r_0 \times 10^{-3}$ (mmol min^{-1})*	Conversion after 180 min (%)
0.10	1.9	66
0.15	3.8	99
0.20	1.9	96

*Initial reaction rate (r_0) = C_0-C_t/t (1/m_{cat}). C_0 and C_t are initial and actual concentration of isoprenol, m_{cat} = mass of catalyst and t is time.

reaction was stopped and the catalyst was recovered by filtering and further reused. The reaction conditions were optimized by changing both the temperature and the ratio between isoprenol and isovaleraldehyde. The repeatability of the tests was also investigated using the best catalyst. For this purpose, H-Beta-300 was recovered by filtration and calcined at 400 °C using the following temperature program: 75 min–250 °C, 50 min–250 °C, 65 min–400 °C, 120 min–400 °C, 100 min–25 °C.

For each experiment, a certain amount of every sample was diluted with dimethyl carbonate to be analyzed by a gas chromatograph (Agilent Technologies 6890 N, with an HP-5 column, length 30 m, diameter 0.32 mm, film thickness 0.5 μm) with the following temperature program: 60 °C (5 min) – 3 °C/min – 130 °C – 12 °C/min – 280 °C (10 min) to quantify the conversion of isoprenol, and for some experiments by a gas chromatograph coupled to a mass spectrometer (Agilent Technologies 5973 N) to identify the products with the following temperature program: 60 °C (5 min) – 3 °C/min – 130 °C – 8 °C/min – 200 °C - +12 °C/

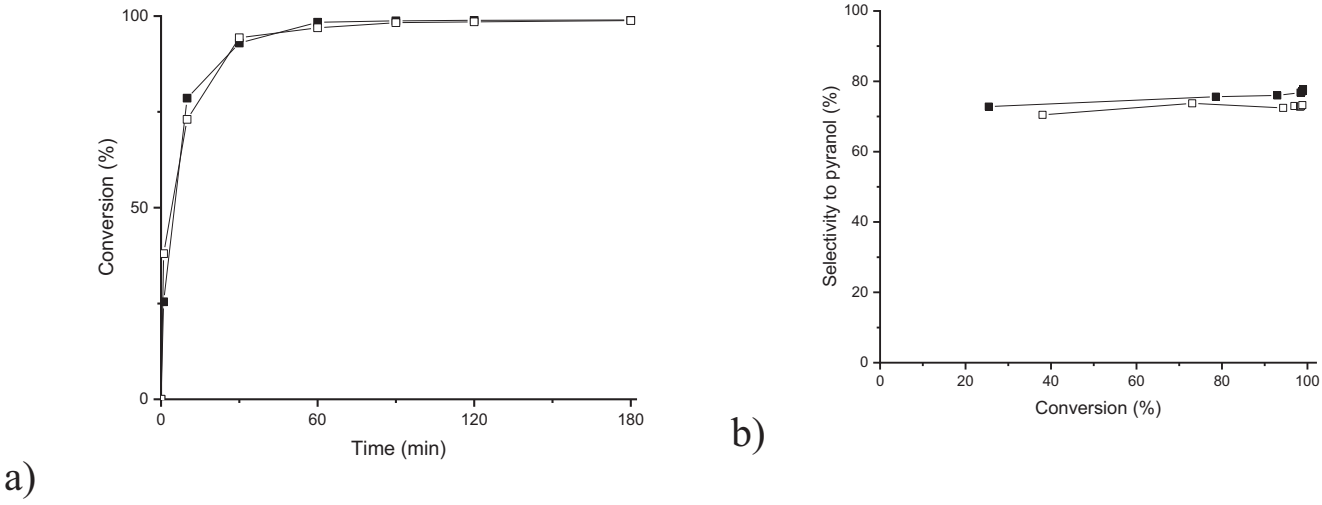

Fig. 4. Conversion of isoprenol as a function of time in the Prins cyclization of isoprenol with isovaleraldehyde at 40 °C with 0.2 M of isoprenol and 1.0 M of isovaleraldehyde over H-Beta-300 catalyst. Notation: experiment 1 (□), experiment 2 (■).

Table 4
Results from Prins cyclization of isoprenol with isovaleraldehyde at 40 °C with 0.2 M of isoprenol and 1.0 M of isovaleraldehyde. Selectivity, cis/trans ratio of pyranols and ratio between different dihydropyrans are given at 50% isoprenol conversion, if not stated otherwise.

Catalyst	Initial rate (mmol min^{-1} g^{-1})	Conversion after 180 min (%)	Selectivity to pyranol (%)	Cis/trans ratio of pyranols (–)	Selectivity to dihydropyrans (%)	DHP(A)/DHP(C) (–)	DHP(B)/DHP(C) (–)
H-Beta-300	0.73	99	72	3.1	21	2.0	0.9
H-Beta-150	0.37	79	65	2.6	27	2.5	1.2
H-Beta-38	0.61	98	60	2.1	33	2.1	1.2
Fe-H-Beta-300	0.21	54	64	2.1	29	2.3	1.2
Fe-H-Beta-38	0.21	52	57	1.7	36	2.2	1.2
H-USY-30	0.99	99	54[a]	1.5 [a]	37[a]	0.7 [a]	0.6[a]
H-USY-30-AT	0.36	98	60	2.1	29[a]	0.8	0.7
H-MMBE-B	0.05	52	54	1.1	39	0.6	0.7
H-MMBE-C	0.08	66	52	1.1	36	0.6	0.7
H-MCM-41	0.2	78	52	1.1	39	0.6	0.7

[a] Conversion 99%.

min – 280 °C (10 min). The GC calibration was made for isoprenol, dehydration products (M = 154 g/mol) and tetrahydropyranol (M = 172 g/mol) with respectively isoprenol, citronellal (M = 154 g/mol) and hydroxycitronellal (M = 172 g/mol), in toluene, as the products are not commercially available and the respective structures are similar (the same molar mass, carbon and oxygen numbers, and similar polarity). For the oxygenated products, a linear response in FID is typically obtained with rather diluted concentrations and thus calibration was performed up to concentrations of 2.4 g/l showing a linear response. The initial mass concentration was typically 17.2 g/l requiring thus 7.2 fold dilution. The mass balance closure was ca. 95%.

2.5. Computational methodology

The optimization of the structures was performed at the DFT level using the hybrid functional of the electronic density Perdew-Burke-Ernzerhoff, PBE (considering computational costs, accuracy and coverage of the results, as it was previously reported) with the 6-311++G(d,p) basis set. All computational runs were carried out in the Gaussian09 program [18]. Well-known standard DFT methods fail to describe the non-local nature of the substances with respect to van der Waals interactions. To account for such interactions, an empirical dispersion correction of Grimme (D3) [19] was considered during the frequencies calculations. After optimization of the structures, additional runs were performed at m062x level (Minnesota functionals) with the same basis set for improving values of energies and for obtaining thermodynamic values of each reaction. The minimal structures were verified with the frequencies values obtained after optimization. Furthermore, such frequencies were also calculated and verified using analytic second derivatives of the energy, which confirm the nature of the stationary point. Solvation effects (dimethylcarbonate) were included and computed at the same level of theory on the optimized structured towards the conductor-like polarizable continuum model (CPCM) implemented in the Gaussian09 package. This model uses several cavity models to compute values of thermodynamic energies being of relatively low computational costs. Particularly, the solute molecule is embedded into a cavity surrounded by a dielectric constant of permittivity ε which ensures continuity and robustness of the reaction [20]. Temperature of the computational runs was 40 °C reflecting the experimental data.

3. Results and discussion

3.1. Catalyst characterization results

The texture of the catalysts was studied by SEM, TEM and nitrogen adsorption. The results from SEM show that the crystallite size of H-Beta-300 was rather small, *ca.* 58 nm and it form clusters of several particles (Fig. 2a). On the other hand, the crystallite size of H-Beta-150 is 33 nm and the small particles are aggregated to larger ones. H-Beta-38 contains large aggregates of maximally 1 μm (Fig. 2c). The structures of iron modified Fe-Beta-300 and Fe-Beta-38 look like similar as the structure of the parent materials (Fig. 2d,e). The images of the parent H-USY-30 zeolite show the crystalline nature of the material and the presence of some mesopores, in line with its manufacturing method (Fig. 2f). Alkaline treatment was effective in increasing the mesoporosity of the zeolite, while substantially retaining the crystallinity of the microporous framework and the overall particle size (Fig. 2g). However, the surface is not very smooth in some places showing clearly the effect of alkali leaching.

TEM image of H-Beta-300 shows that crystallites are from 10 nm upwards and the zeolite structure is clearly visible (Fig. 3a). The structure of H-Beta-150 is rather similar to that of H-Beta-300 (Fig. 3a, b, d), while the particle size of H-Beta-38 is large, e.g. ca. 120 nm (Fig. 3c). Rather larger Fe particles (90 nm) are visible on H-Beta-300 (Fig. 3e), while much smaller iron particles in the range of 7–20 nm can be found on Fe-H-Beta-38 (Fig. 3f), which has higher acidity. TEM images of MM-BE-B and MM-BE-C in [16] show clearly regular periodicity and uniform pores.

Specific surface areas for zeolites decreased as follows: H-Beta-38 > H-USY-30 > H-Beta-300 > H-Beta-150 while Fe-modified H-Beta catalysts exhibited as expected lower specific surface area than their parent forms (Table 1). The median pore width for all zeolites was in the range of 0.66 to 0.80 nm, which is typical for this kind of materials. Meso to micropore ratio increased from H-Beta-300 to H-beta 25 with decreasing Si/Al ratio, although for H-Beta-38 this was not determined. The pore diameter increased from 0.658 nm of H-Beta-zeolites to 0.77 nm for H-USY-30 and the alkali treated H-USY-AT exhibited a slightly larger pore diameter. For mesoporous materials, the highest specific surface area was observed for H-MCM-41 followed by H-MMBE-B and HMMBE-C. The pore sizes of mesoporous H-MMBEs and H-MCM-41 were equal or larger than 3 nm.

The results from catalyst acidity measurements (Table 2) show that H-Beta-38 exhibited the highest total acidity and also a high concentration of strong acid sites. The Brønsted to Lewis acid ratio was also the highest for H-Beta-38, while H-Beta-300 and H-Beta-150 as expected exhibited a lower amount of Brønsted acid sites. Acidity of H-USY-30 was also lower than H-Beta-150 and 38. The amounts of Brønsted and Lewis acid sites in the alkali treated H-USY-AT were 63% and 86% of those found in the parent H-USY. Furthermore, this material exhibited no strong acid sites. Mesoporous MMBE B, MMBE C and H-MCM-41 displayed mild acidity, although the highest amount of strong acid sites among these three catalysts was present in H-MCM-41. The acidity of H-MMBE was lower than

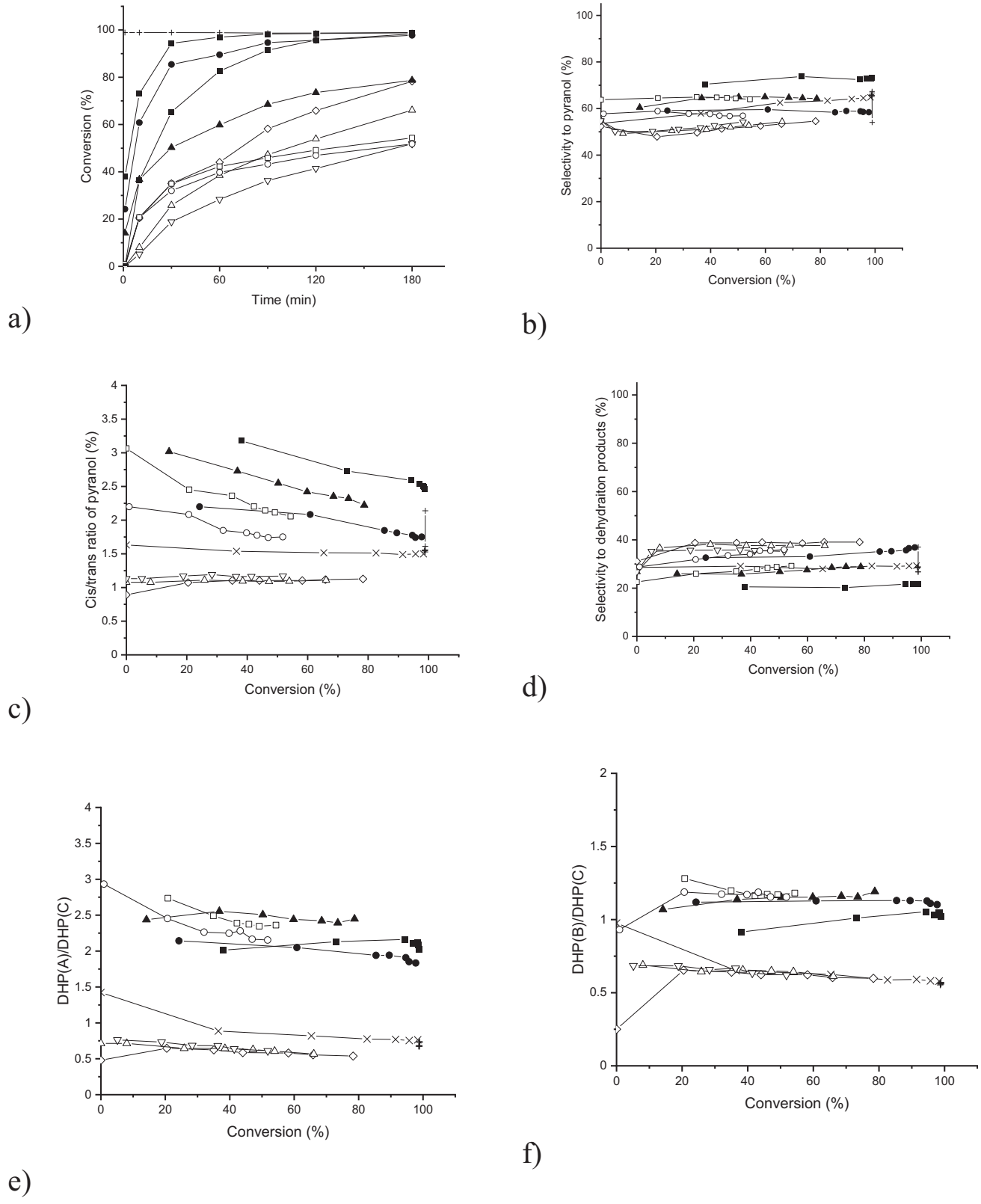

Fig. 5. a) Conversion of isoprenol as a function of time, b) selectivity to pyranol, c) cis/trans ratio of pyranols, d) selectivity to dehydration products, e) DHP(A)/DHP(B) ratio, f) DHP(B)/DHP(C) ratio as a function of conversion in the Prins cyclisation of isoprenol with isovaleraldehyde at 40 °C with 0.2 M of isoprenol and 1.0 M of isovaleraldehyde. Notation: H-Beta-300 (■), H-Beta-150 (▲), H-Beta-38 (●), H-Beta-25 (▼), Fe-Beta-300 (□) , Fe-Beta-38 (o), HUSY-30 (+), HUSY-30-AT (x), MMBE B (X), MMBE C (Δ) and H-MCM-41 (M).

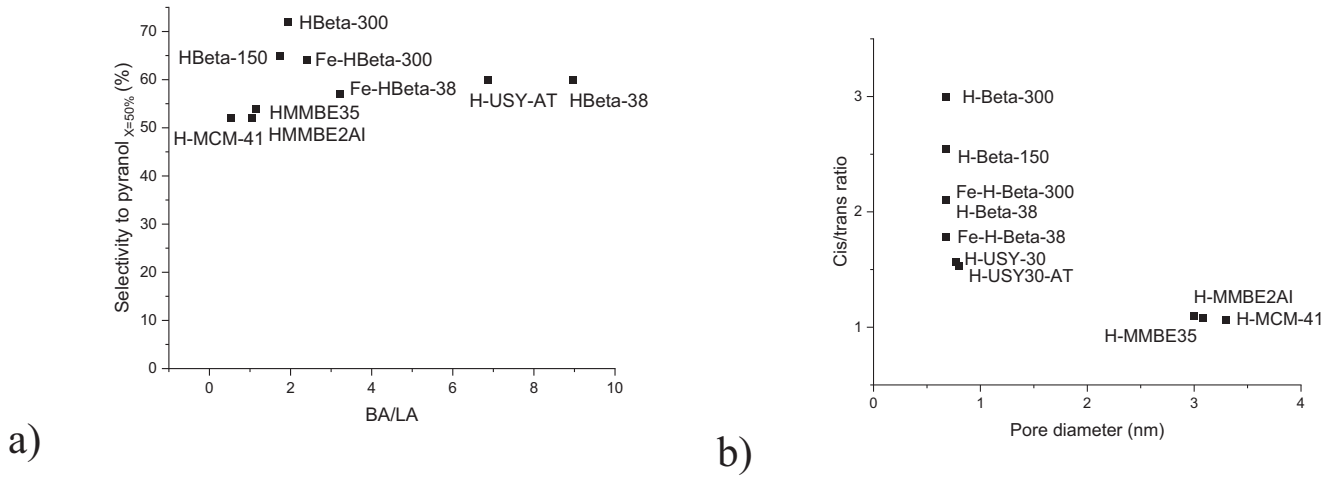

Fig. 6. a) Selectivity to pyranols as a function of the BA/LA ratio and b) cis/trans ratio of tetrahydropyranols at 50% conversion over different catalysts in the Prins cyclisation of isoprenol with isovaleraldehyde at 40 °C with 0.2 M of isoprenol and 1.0 M of isovaleraldehyde. Notation: Brønsted acid sites BA, Lewis acid sites LA.

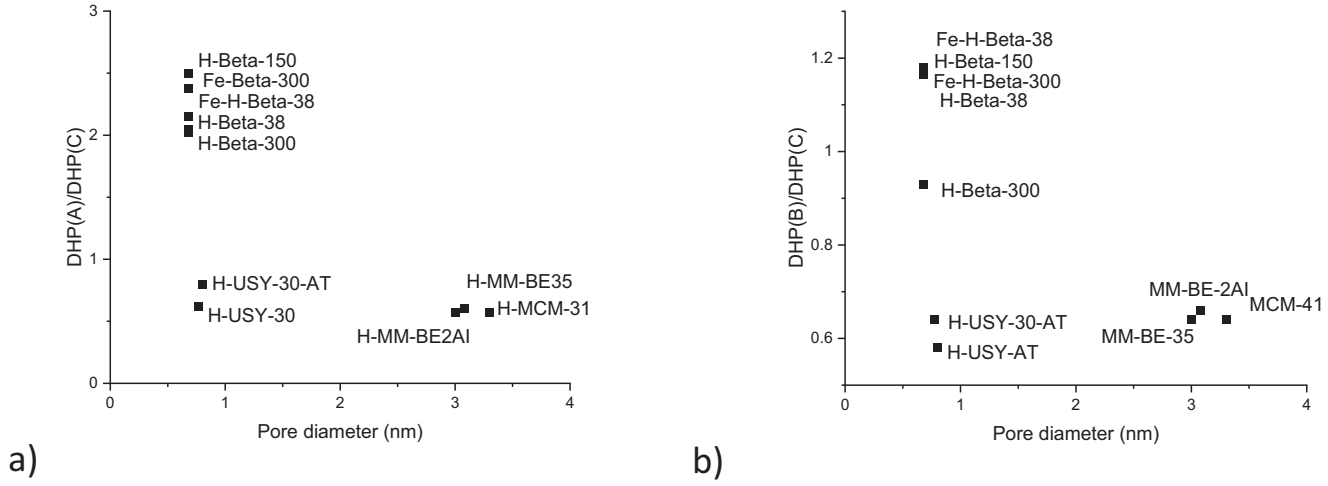

Fig. 7. a) DHP(A)/DHP(C) and b) DHP(B)/DHP(C) ratios as a function of average pore size.

that for H-MMBE C as expected, because the former catalyst contained 1.5 wt% Al and the latter one 3.9 wt% [26].

3.2. Catalytic Prins cyclisation

3.2.1. Effect of catalyst mass

In the preliminary experiments, the mass of H-Beta-150 was varied to verify that the experiments are performed in the kinetic regime. In this series, the Prins cyclisation of isoprenol with isovaleraldehyde was performed using the molar ratio of isoprenol to isovaleraldehyde of 1:5 at 40 °C in dimethylcarbonate as a solvent. For these conditions the catalyst mass was varied from 0.1 to 0.2 g. The results showed that the initial rate increased twofold when the catalyst mass was increased by a factor of 1.5 (Table 3). Almost complete conversion was achieved after 3 h with both 0.15 and 0.20 g of catalyst. Considering these results and the values of the initial reaction rates further experiments were conducted with 0.15 g of catalyst.

Repeatability of the results was investigated via performing experiments in Prins cyclisation using the same reaction conditions described above for H-Beta-300 catalyst. The data gathered for the conversion of isoprenol as a function of time in two experiments (Fig. 4) illustrated that there is a complete overlapping of concentration profiles confirming that the results are reproducible. Comparison of the initial rates for the repeated tests with H-Beta-300 demonstrated that the difference was below 5%.

3.2.2. Results from catalyst screening

Different H-Beta zeolites with varying Si/Al ratio as well as H-USY-30 and its alkali-treated counterpart, H-USY-30-AT, were tested in the Prins cyclization of isoprenol with isovaleraldehyde. In addition to mesoporous H-USY-30-AT, also other mesoporous catalysts including H-MCM-41 and two different hybrid MCM-41-Beta- zeolite catalysts, were evaluated in the same reaction to verify the effect of the pore size, surface area and acidity. The results revealed that the highest initial rate during the first 10 min were obtained with H-USY-30 and H-Beta-300 (Table 3), which both exhibited a rather mild acidity, as well as a small amount of strong acid sites (Table 2). For the mesoporous catalysts, which contain no strong acid sites, the initial reaction rate was very low (below 0.2 mmol min^{-1} g^{-1}). This is in line with [7], stating that the initial reaction rate increased upon increasing the amount of strong acid sites.

The reaction rates after prolonged reaction times declined for iron-modified zeolites, while very high rates and conversion levels were obtained for H-Beta-300, H-USY-30, H-Beta-38, and H-USY-

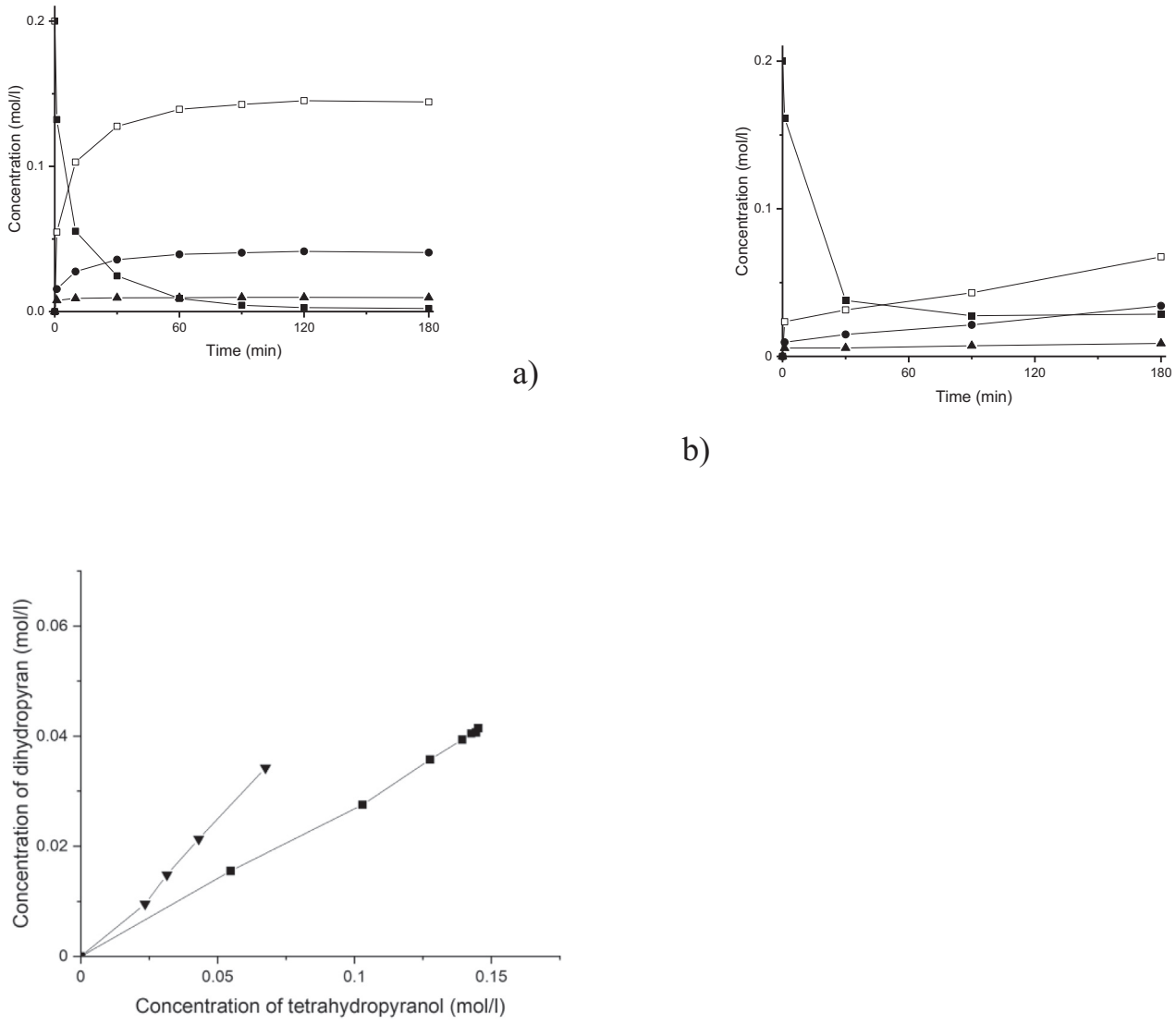

Fig. 8. Concentration profiles of isoprenol (■), tetrahydropyranol (□), dihydropyran (●) and oligomer (▲) in the Prins cyclisation of isoprenol with isovaleraldehyde at 40 °C with 0.2 M of isoprenol and 1.0 M of isovaleraldehyde at 40 °C over a) H-Beta-300 and b) H-Beta-150. c) Concentration of dihydropyrans as a function of the concentration of tetrahydropyranol over H-Beta-300 (■) and H-Beta-150 (▼).

30-AT (Table 4 and Fig. 5). The iron modified zeolites gave much lower conversion levels than their non-modified counterparts, most probably due to their lower amount of strong acid sites (in both Lewis and Bronsted acid sites) (Table 2). A rate decline for H-Beta-150 after 10 min was somewhat unexpected considering acidity of this zeolite (Fig. 5a).

For mesoporous catalysts, such as H-MCM-41-F, MMBE-B and MMBE-C exhibited higher rates even at prolonged reaction times. The conversion of these catalysts increased as follows: H-MMBE-B < HMMBE-C < H-MCM-41, corresponding to the order of acidity (Table 4).

Selectivity to tetrahydropyranols as a function of conversion is typically rather constant (Fig. 5b) pointing out on their parallel formation with the corresponding dehydrated products with a common intermediate. The highest selectivity to pyranols was obtained with H-Beta-300 (72%, Table 4). Other non-modified zeolites attained an only slightly lower selectivity, while, mesoporous mildly acidic catalysts gave lower pyranol selectivity (Fig. 5b). The current results differ from those reported by Sidorenko et al. [7], when a hemiacetal was found as an intermediate over halloysite clay as a catalyst in cyclohexane as a solvent at 90 °C. In that case [7] selectivity to tetrahydropyranols was ca. 10% for isoprenol conversion of up to 65%, after which it rapidly increased reaching finally ca. 54% at 82% conversion. The reason for absence of the hemiacetal formation in the current work is stronger acidity of zeolites and mesoporous catalysts, compared to halloysite clays.

The desired pyranol product is the *cis* form with H-Beta-300 displaying the highest cis/trans pyranol ratio of 3.1. This ratio decreased as a function of conversion for microporous catalysts indicating that the *cis* isomer reacted further more rapidly than the *trans* isomer, while this ratio was ca. 1.1 for mesoporous catalysts (Fig. 5c). As a comparison to [7] the *cis/trans* ratio increased slightly with increasing conversion from 1.5 to 2, when mesoporous K-10 clay was used as a heterogeneous catalyst [7]. Furthermore, cis/trans ratio of 2:1 was obtained over mesoporous $H_3PW_{12}O_{40}/SiO_2$ catalyst [9].

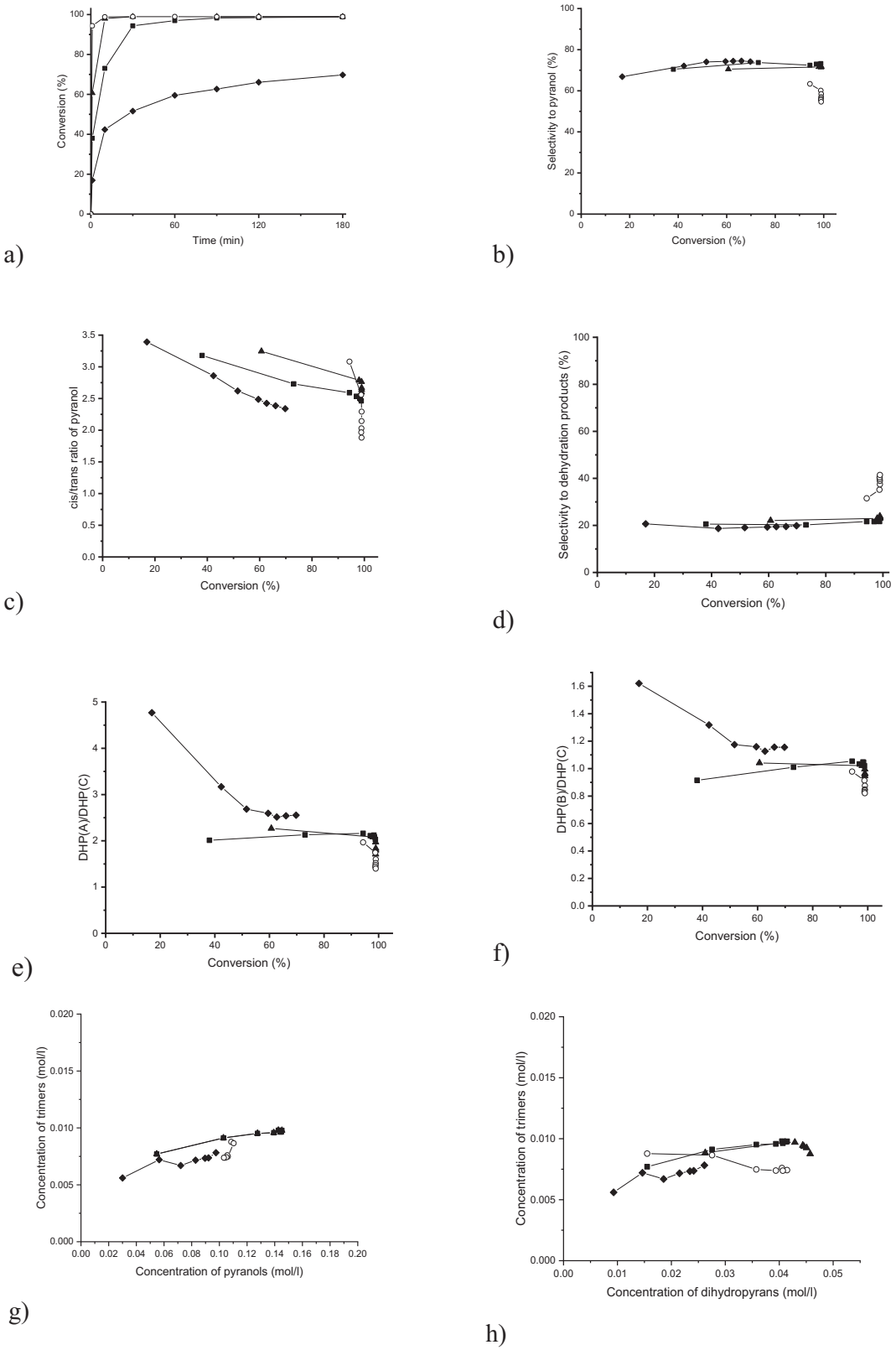

Fig. 9. Effect of temperature on a) isoprenol conversion, b) selectivity to pyranol, c) cis/trans ratio of pyranols, d) DHP(A)/DHP(C) ratio, e) DHP(B)/DHP(C) ratio as a function of conversion, g) concentration of trimers vs pyranols and h) concentration of trimers vs dihydropyrans in the Prins cyclization of isoprenol with isovaleraldehyde at 40 °C with 0.2 M of isoprenol and 1.0 M of isovaleraldehyde over H-Beta-300. Notation: 24 °C (◆), 40 °C (■), 60° C (▲) and 80 °C (o).

The high cis/trans ratio of tetrahydropyranols is consistent with the values of $GAP_{HOMO\text{-}LUMO}$ calculated using computational chemistry. The highest occupied molecular orbital (HOMO)-lowest unoccupied molecular orbital (LUMO) energy separation has been used along the years for many reacting systems as a simple indicator of kinetic stability. A large HOMO-LUMO gap corresponds to

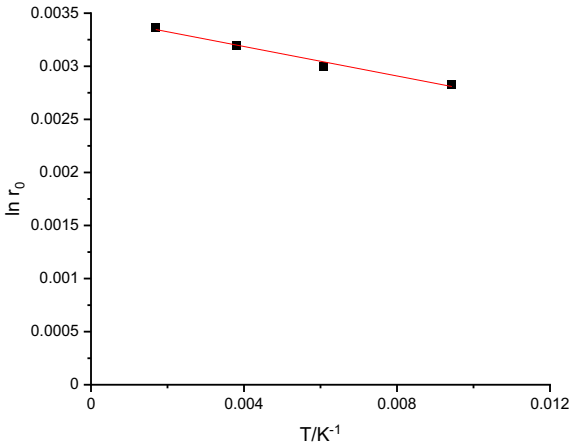

Fig. 10. Activation energy calculated from the initial rates r_0 in the Prins cyclization of isoprenol with isovaleraldehyde between 40 °C and 80 °C with 0.2 M of isoprenol and 1.0 M of isovaleraldehyde over H-Beta-300.

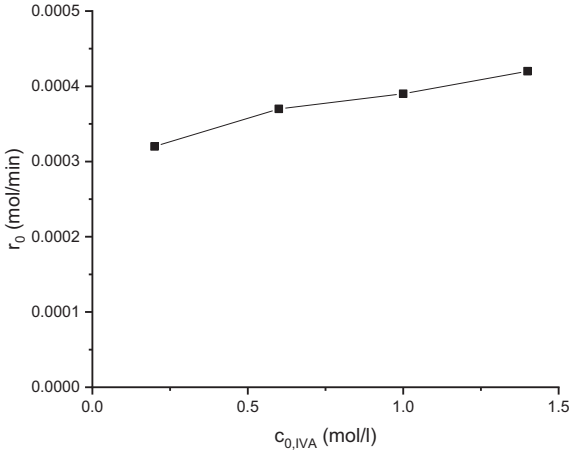

Fig. 11. Initial reaction rate for transformation of isoprenol during the first 10 min reaction time as a function of isovaleraldehyde concentration. The initial concentration of IP is 0.2 M.

high kinetic stability and low chemical reactivity, as formation of an activation complex is energetically unfavourable when electrons are taken from a low-lying HOMO and added to a high-lying LUMO. Subsequently a small value of $GAP_{HOMO-LUMO}$ indicates that the molecule is more reactive while a large value of GAP is indicative of less reactivity of the system [27]. In this way, the value of $GAP_{HOMO-LUMO}$ for *cis*-THP was of 10.42 eV while for *trans*-THP was of 10.47 giving a difference of 0.05 eV between those molecules. This result implies that the *cis* configuration reacts more rapidly than the *trans*- isomer being even quantitatively in line with the experimental evidences of this study.

The difference of $GAP_{HOMO-LUMO}$ for *cis*- and *trans*- THP is however, not that high and for mesoporous catalysts the cis/trans ratio remained constant with increasing conversion (Fig. 5c). As a comparison with the literature, a halloysite clay gave about the same cis/trans pyranols ratio, i.e. 3.0 [7], as the maximum one in the current case.

From the cis/trans pyranols ratio at 50% conversion as a function of the catalyst pore diameter (Fig. 6a), it can be observed that this ratio decreased rapidly upon increasing the pore diameter (Fig. 6b).

A comparison of the reactants and products molecular sizes calculated by Gaussian G09, B3LYP/6-311g(d,p)//M-062X/6-311g(d,p), including empirical dispersion (gd3, in the case of the first optimization with B3LYP as the electronic functional) with the pore sizes of different catalysts, illustrates that the pores of H-Beta- zeolites are smaller than the size of tetrahydropyranol, which is exceeding 0.9 nm, being 0.939 nm for *trans* and 0.906 nm for *cis* isomer. This indicates that the reaction might proceed mainly on the external surface of the catalyst. Furthermore, the cross section of dihydropyrans (DHPa-c) is 0.91–0.94 nm while the pore sizes of H-USY-30 and H-USY-30-AT are 0.77 nm and 0.8 nm, respectively. Nevertheless penetration by the reactants and products cannot be excluded as materials with larger pores were more beneficial for the formation of *trans* pyranol bearing a larger cross section. Namely, the *trans/cis* ratio of pyranols was higher for USY catalysts in comparison to H-Beta catalysts (Fig. 5c).

Selectivity to DHPs was rather constant with increasing conversion (Fig. 5d) pointing out on the parallel formation of DHP from the same intermediate, which give THP. The ratio between A:B:C (isomers of DHP) obtained over H-Beta-300 was 2.1:0.95:1, while for mesoporous H-MCM-41 it was 0.59: 0.62: 1 at 50% conversion. This result is in accordance with the work of [9], reporting that mesoporous phosphortungstic acid catalysts gave the ratio of dihydropyran A:B:C isomers of 1:1:3. On the other hand, the ratio between different dehydrated products showed an interesting trend, namely the DHP(A)/DHP(C) ratio was higher for microporous catalysts in comparison to the mesoporous catalysts, except for the very strongly acidic H-Beta-25 (Fig. 7a). The same holds for the DHP(B)/DHP(C) ratio (Fig. 7b).

In order to compare kinetics and mechanism of the Prins cyclization of isoprenol with isovaleraldehyde the concentrations of isoprenol and the products were plotted as a function of time showing clearly the H-Beta-300 gave a higher yield of tetrahydopyranol in comparison to H-Beta-150 (Fig. 8). Furthermore, the concentration of dihydropyran was also plotted as a function of tetrahydropyranol in order to detect whether their formation is consecutive. The results show that these products are generated in parallel, with r_{DHP}/r_{THP} being 0.41 for H-Beta-150 while 0.28 for H-Beta-300. In addition, the selectivity to more dihydropyrans was ca. 24% at 70% conversion, while for H-Beta-300 it was only 20%.

3.2.3. Effect of reaction conditions

3.2.3.1. Effect of temperature. The reaction temperature was varied in the range of 24 °C to 80 °C in the Prins cyclization of isoprenol with isovaleraldehyde over H-Beta-300 catalyst (Fig. 9). The activation energy was determined from the initial reaction rate during the first 10 min from the Arrhenius equation being 118 kJ/mol (Fig. 10) with the high quality of the fit R^2 being 0.976. Although effect of temperature was studied in [28] in Prins cyclization of isopulegol with acetone, activation energy was not reported.

The selectivity to tetrahydropyranol decreased slightly with increasing temperature, while at the same time the cis/trans ratio of pyranols increased with increasing temperature (Fig. 9b). Analogously, in [9] selectivity to tetrahydropyranols decreased with increasing temperature. Especially at 80 °C the dehydration of tetrahydropyranol was enhanced (Fig. 9d). Interestingly the highest ratios of DHP(A)/DHP(C) and DHP(B)/DHP(C) were found at 24 °C (Fig. 9e,f). Detailed analysis of the formation of different dihydropyrans at different temperatures is not given in [9], but only selectivity of all dihydropyrans, which increased with increasing temperature.

3.2.3.2. Effect of the ratio between isoprenol and isovaleraldehyde. The molar ratio between isoprenol to isovaleraldehyde in the Prins cyclisation of them over H-Beta-300 was varied in the

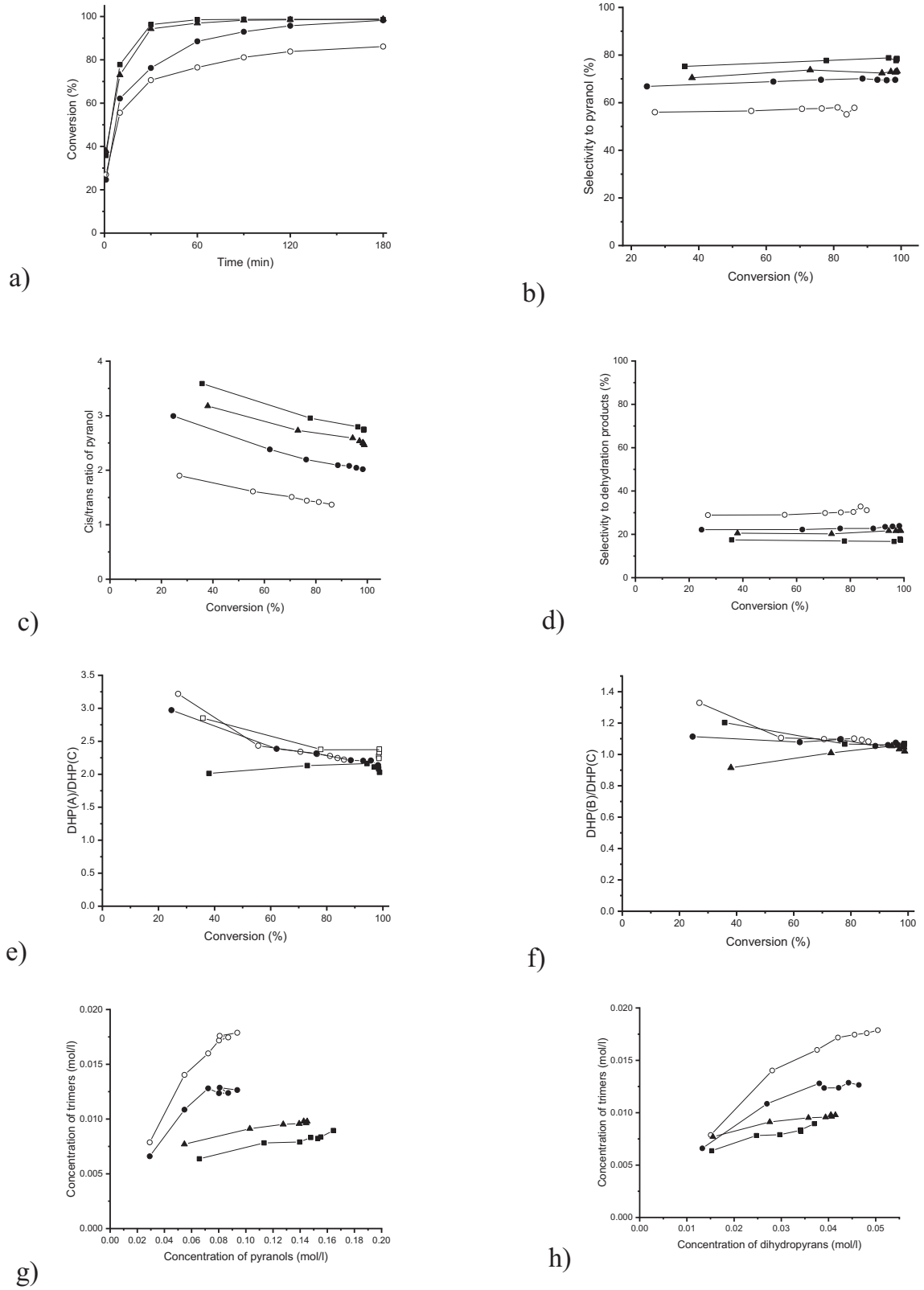

Fig. 12. Effect of the initial ratio of isoprenol to isovaleraldehyde on a) isoprenol conversion, b) selectivity to pyranols, c) *cis*/*trans* ratio of pyranols, d) selectivity to dehydration products, e) DHP(A)/DHP(C) ratio and f) DHP(B)/DHP(C) ratio as a function of conversion, g) concentration of trimers vs pyranols and h) concentration of trimers vs dihydropyrans in the Prins cyclisation of isoprenol with isovaleraldehyde at 40 °C over H-Beta-300. Notation: 0.2 M IP and 0.2 M IVA (o), 0.2 M IP and 0.6 M IVA (●), 0.2 M IP and 1.0 M IVA (▲) and 0.2 M IP and 1.4 M IVA (■) molar ratio of isoprenol to isovaleraldehyde.

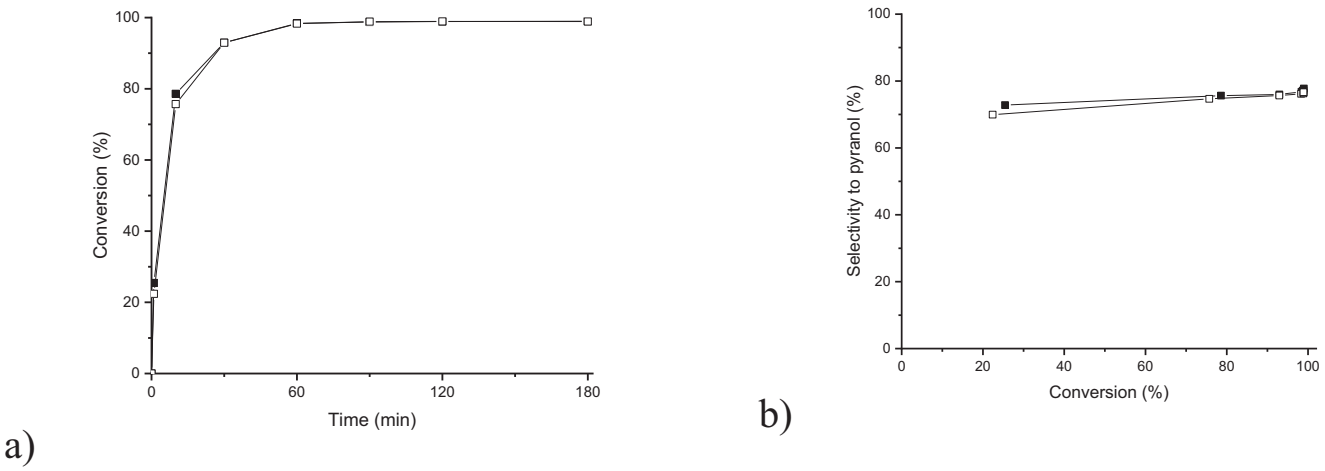

Fig. 13. a) Conversion of isoprenol and b) selectivity to pyranols over a fresh (■) and reused H-Beta-300 after catalyst calcination (□). Reaction conditions: 40 °C with 0.2 M of isoprenol and 1.0 M of isovaleraldehyde dimethylcarbonate as a solvent.

range of 1 to 7 by increasing the amount of isovaleraldehyde. The results showed that the initial rate for transformations of isoprenol increased by ca. 30% when increasing the initial concentration of isovaleraldehyde from 0.2 to 1.4 mol/L (Fig. 11) with a small value of the slope indicating a low reaction order to isovaleraldehyde.

These results are in line with the observations regarding the final conversion, namely that the 1:1 M ratio gave 86% conversion in 3 h (Fig. 12 a), while ca. 98–99% conversion was obtained with the molar ratios of isoprenol to isovaleraldehyde of 3 to 7.

The selectivity to tetrahydropyranol decreased with increasing the molar ratio of isovaleraldehyde to isoprenol (Fig. 12b), while selectivity to sum of the dehydration products (DHP(A) + DHP(B) + DHP(C)) increased with increasing this ratio (Fig. 12d) which is probably related to different involvement of the substrates (isovaleraldehyde and isoprenol) in side reactions occurring on the acid sites of the catalyst. An analogous trend was observed in [9] in the same reaction over a heterogeneous phosphotungstic acid catalyst.

Experimental data indicated an increase of the *cis/trans* ratio for tetrahydropyranol (Fig. 12c) upon elevation of the molar ratio of isovaleraldehyde to isoprenol.

The ratio between different dihydropyrans changed also with changing the initial ratio of the reactants. With a lower ratio of isoprenol to isovaleraldehyde, the ratio between DHP(A)/DHP(C) was the highest at low conversion levels being in the range of 3.0–3.3, while this trend was not very obvious for the DHP(B)/DHP(C) ratio (Fig. 12e). At high conversion levels, the differences in both DHP (A)/DHP(C) and DHP(B)/DHP(C) were very small corresponding to the values of 2.1–2.2 and ca. 1.0, respectively (Fig. 12e, f). In the consecutive step trimeric compounds with the molecular mass of 224 g/mol were observed to be formed (Fig. S1). The MS pattern of this trimeric compound clearly shows that it has as a structural motif DHP to which isoprenol is added via condensation. The amount of T(C) increased with decreasing concentration of isovaleraldehyde and it was typically 3.6 to 4.5 fold higher than the amount of T(B) followed by only small amounts of T(A) indicating that a high initial isoprenol concentration promoted formation of trimeric compounds.

Apparently, the distribution of DHP isomers and THP stereoisomers depends on the isovaleraldehyde to isoprenol ratio, influencing the type and surface concentration of carbocations, which further transformations define formation of one stereoisomer over another one. Preliminary theoretical analysis in included in the current work, however, a dedicated mechanistic investigation is apparently needed in the future.

3.2.4. Results from catalyst reusability

The best performing catalyst, H-Beta-300 was used in two consecutive experiments with the spent catalyst from the first run calcined at 400 °C in air prior to the second experiment. The results indicate that the catalyst activity and selectivity were fully recovered after this treatment (Fig. 13) showing that the material is robust and reusable for the synthesis of the desired tetrahydropyranols from isovaleraldehyde and isoprenol.

3.2.5. Reaction pathways

DFT calculations were performed to elucidate the mechanistic aspects of the reaction between isovaleraldehyde and isoprenol. Two different reaction pathways were investigated including formation of dehydration products from tetrahydropyranol in a consecutive manner or alternatively via a parallel formation of THP and DHP. In the first case H_3O^+ was considered as an acidic catalyst without mimicking the structure of zeolites and mesoporous materials. This species were chosen because they account for the Brønsted type of acid sites present in the catalysts. Fig. 14a shows the reaction profile for the synthesis of tetrahydropyranol isomers (*cis/trans*) and their dehydrated products. It seems that both isoprenol and isovaleraldehyde react together to obtain a carbocation with a difference of 17.6 kJ/mol. Then, elimination of water from the carbocation **B** gives a new substance **C** with at least 16.7 kJ/mol of difference, being thus more spontaneous and energetically favorable.

For carbocation C, the positive charge is localized on the oxygen atom because of the *anti*-elimination of water. Because of the presence of an intermolecular double C-C bond and a good electrophile group (C = O^+), further cyclization occurs more rapidly leading to a pyranol like carbocation (**D**). In this case, a difference of 25.1 kJ/mol allows to obtain a substance that is thermodynamically favorable. Finally, addition of water together with the acidic proton gives both *cis* and *trans*-configurations of THP. As it is shown in Fig. 14a it appears that both ***Dc*** and ***Db*** products are slightly more thermodynamically favorable than *cis/trans* THP.

In this research, it was shown that further synthesis of the dehydrated products occurred in parallel to tetrahydropyranol (Fig. 8c). The hypothesis of a direct formation of DHP from the carbocation D would be in line with suggestions advanced in [9] regarding the Prins reaction of isovaleraldehyde with isoprenol. Such suggestion implies parallel formation of THP and DHP (Fig. 14b). This mechanism involves aldehyde protonation over Brønsted acids and when it is reacting with isoprenol a protonated hemiacetal will be formed. An oxocarbenium ion is formed via

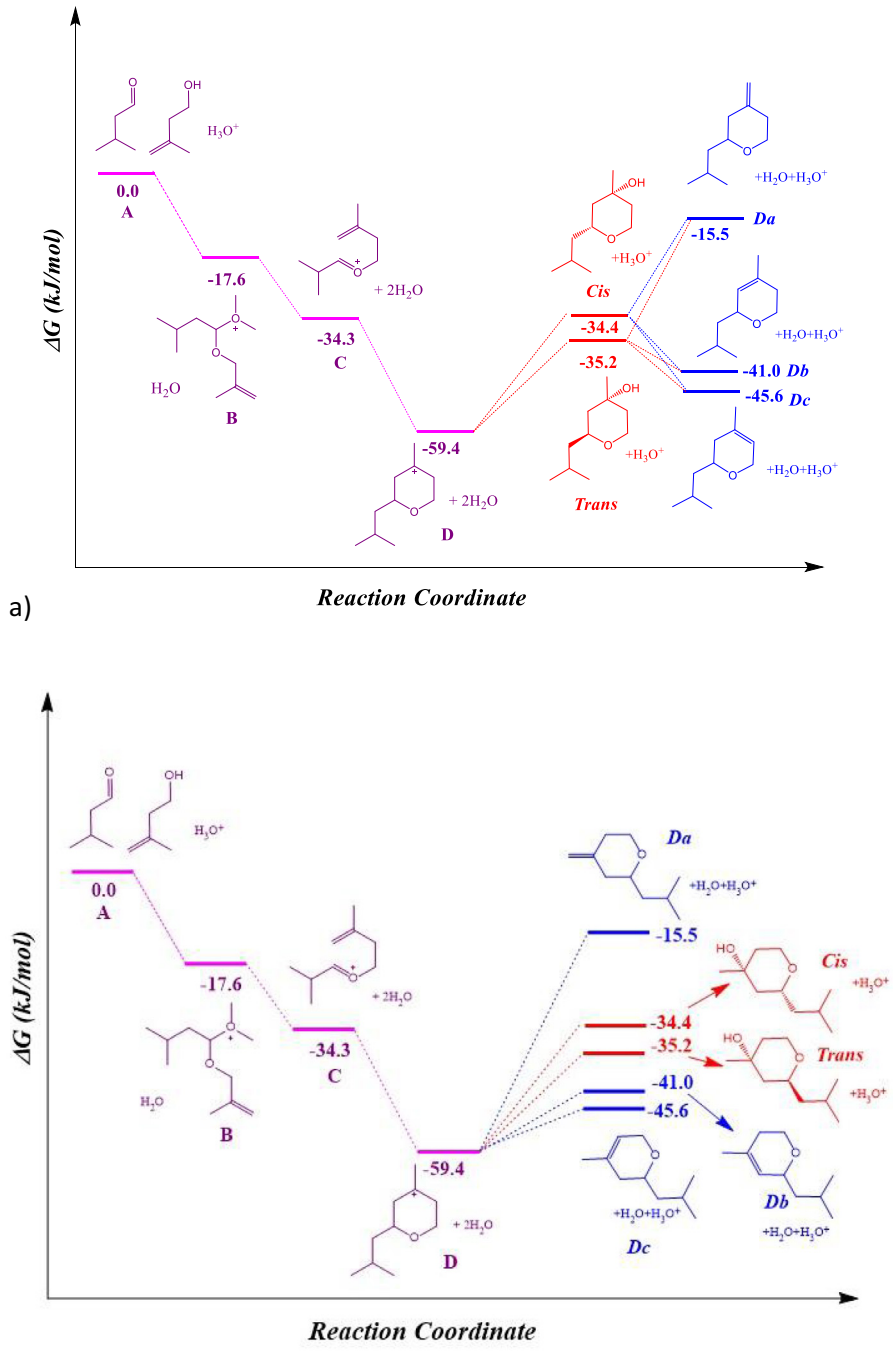

Fig. 14. DFT reaction scheme for the consecutive formation of tetrahydropyranol and dehydrated pyranol substances and b) parallel route according to [9] using H_3O^+ as an acidic catalyst.

water elimination from the protonated hemiacetal. Thereafter, an intermediate C is formed when C=C double bonds will interact in B. The intermediate C can either react with water forming the desired THP or alternatively undergo proton elimination when dihydropyrans are formed.

4. Conclusions

Several parent and metal modified Beta zeolites with varying SiO_2/Al_2O_3 ratio together with parent and alkali treated H-USY zeolites and mesoporous catalysts were prepared and tested in synthesis of tetrahydropyranol (THP) via Prins cyclization starting from isovaleraldehyde and isoprenol in a batch reactor. In addition to catalyst screening also the effect of temperature, amounts of reactants and the catalyst reuse were investigated for the best catalyst to explore the influence of reaction parameters. The reaction kinetics was also investigated giving besides initial rates also detailed profiles of THP, dehydrated products and trimers at different isovaleraldehyde to isoprenol ratios. The results form Prins cyclization revealed that the best catalyst was a microporous H-Beta-300 zeolite giving 72% selectivity to the desired product at 99% conversion at 40 °C in dimethylcarbonate as a solvent. For this catalyst repeatability and catalyst reuse were successfully confirmed. The *cis/trans* ratio of the desired tetrahydropyranols at 50% conversion was much higher for microporous catalysts than

for mesoporous ones It was also shown that an optimum ratio of Brønsted to Lewis acids gave the highest selectivity to tetrahydropyranol at 50% conversion. It was also proposed by DFT calculations that the reaction might proceed on the external surface of the catalyst, because the size of tetrahydropyranol is larger than the pore size of H-Beta zeolite. Parallel formation of tetrahydropyranol and dihydropyran was observed and theoretically confirmed by DFT calculations.

The effect of reaction conditions, e.g. temperature and the molar ratio of reactants was also investigated for H-Beta-300. Activation energy for Prins cyclization of isovaleraldehyde with isoprenol, previously not available in the literature, was determined to be 118 kJ/mol, previously. Selectivity to tetrahydropyranols over H-Beta-300 was not affected by temperature in the range of 24 – 60 °C, while at 80 °C lower values were recorded due to formation of the undesired dehydration products. When changing the initial ratio of reactants, it was found the initial rate for isoprenol transformation increased by 30% when increasing the isovaleraldehyde to isoprenol ratio from 1:1 to 1:7. At the same time selectivity to tetrahydropyranol increased with increasing isovaleraldehyde to isoprenol. In addition to formation of tetrahydropyranol and dihydropyrans also trimeric products with the molecular mass of 224 g/mol were also formed. Their amount was the highest with an equimolar amount of isovaleraldehyde and isoprenol indicating that isoprenol might react further with the dehydrated product.

Declaration of Competing Interest

The authors declare that they have no known competing financial interests or personal relationships that could have appeared to influence the work reported in this paper.

Acknowledgements

Electron microscopy samples were processed and analyzed in the Electron Microscopy Laboratory, Institute of Biomedicine, University of Turku, which receives financial support from Biocenter Finland. J.E. S-V is grateful Pontificia Universidad Javeriana for the “Apoyo a Estancias Postdoctorales” (2020-2021) program.

References

[1] G.P. More, M. Rane, S.V. Bhat, Efficient Prins cyclization in environmentally benign method using ion exchange resin catalyst, Green Chem. Lett. Rev. 5 (1) (2012) 13–17.
[2] F. Doro, N. Akeroyd, F. Schiet, A. Narula, The Prins reaction in the fragrance industry: 100th Anniversary (1919–2019), Angew. Chem. 131 (22) (2019) 7248–7253.
[3] A. Macedo, E.P. Wendler, A.A.D. Santos, J. Zukerman-Schpector, E.R. Tiekink, Solvent-free catalysed synthesis of tetrahydropyran odorants: the role of SiO_2, J. Braz. Chem. Soc. 21 (8) (2010) 1563–1571.
[4] E. Vyskočilová, M. Krátká, M. Veselý, E. Vrbková, L. Červený, Prins cyclization for the preparation of 2-isobutyl-4-methyl-tetrahydro-2H-pyran-4-ol using supported heteropoly acids, Res. Chem. Intermed. 42 (9) (2016) 6991–7003.
[5] E. Vyskočilová, L. Rezková, E. Vrbková, I. Paterová, L. Červený, Contribution to elucidation of the mechanism of preparation of 2-isobutyl-4-methyltetrahydro-2H-pyran-4-ol, Res. Chem. Intermed. 42 (2) (2016) 725–733.
[6] L. Sekerová, E. Vyskočilová, J.S. Fantova, I. Paterová, J. Krupka, L. Červený, Preparation of 2-isobutyl-4-methyltetrahydro-2 H-pyran-4-ol via Prins cyclization using Fe-modified silica, Res. Chem. Intermed. 43 (8) (2017) 4943–4958.
[7] A.Y. Sidorenko, Y.M. Kurban, A. Aho, Z.V. Ihnatovich, T.F. Kuznetsova, I. Heinmaa, D.Y. Murzin, V.E. Agabekov, Solvent-free synthesis of tetrahydropyran alcohols over acid-modified clays, Mol. Catal. 499 (2021) 111306, https://doi.org/10.1016/j.mcat.2020.111306.
[8] T. Stork, M. Dehn, K. Ebel, K. Beck, A. Salden, R. Pelzer, Production of 2-subtituted 4-hydroxy-4-methyltetrahydropyrans having stable odoriferous quality, US2017, 0037021 A1.
[9] A.L.P. de Meireles, K.A. da Silva Rocha, E.F. Kozhevnikova, I.V. Kozhevnikov, E.V. Gusevskaya, Heteropoly acid catalysts in Prins cyclization for the synthesis of Florol®, Mol. Catal. 502 (2021) 111382, https://doi.org/10.1016/j.mcat.2020.111382.
[11] S. Wang, B.B. Uzoejinwa, A.-F. Abomohra, Q. Wang, Z. He, Y. Feng, B.o. Zhang, C.-W. Hui, Characterization and pyrolysis behavior of the green microalga Micractinium conductrix grown in lab-scale tubular photobioreactor using Py-GC/MS and TGA/MS, J. Anal. Appl. Pyrol. 135 (2018) 340–349.
[12] E. Vyskočilová, L. Sekerová, I. Paterová, J. Krupka, M. Veselý, L. Červený, Characterization and use of MoO_3 modified alumosilicates in Prins cyclization of isoprenol and isovaleraldehyde, J. Porous Mater. 25 (1) (2018) 273–281.
[13] A. Kang, D. Mendez-Perez, E.-B. Goh, E.E.K. Baidoo, V.T. Benites, H.R. Beller, J.D. Keasling, P.D. Adams, A. Mukhopadhyay, T.S. Lee, Optimization of the IPP-bypass mevalonate pathway and fed-batch fermentation for the production of isoprenol in Escherichia coli, Metab. Eng. 56 (2019) 85–96.
[14] A. Abate, E. Brenna, C. Fuganti, F.G. Gatti, S. Serra, Lipase-catalysed preparation of enantiomerically enriched odorants, J. Mol. Catal. B Enzym. 32 (1-2) (2004) 33–51.
[15] G. Gralla, K. Beck, M. Klos, U. Griesbach, Process for preparation and isolation of 2-substituted tetrahydropyranols, US 8791276 B2, 2014.
[16] N. Kumar, P. Mäki-Arvela, S. Fugleberg, T. Yläsalmi, J. Villegas, T. Heikkilä, A.R. Leino, M. Tiitta, H. Österholm, T. Salmi, D. Murzin, Dimerization of 1-butene in liquid phase over H-NK-MM-BEA type embedded mesoporous materials, Catal. Sustain. Energy 1 (2013) (2012) 1–10.
[17] C.A. Emeis, Determination of integrated molar extinction coefficients for infrared absorption bands of pyridine adsorbed on solid acid catalysts, J. Catal. 141 (2) (1993) 347–354.
[18] K.E. Riley, B.T. Op't Holt, K.M. Merz, Critical assessment of the performance of density functional methods for several atomic and molecular properties, J. Chem. Theory Comput. 3 (2007) 407–433.
[19] W. Reckien, F. Janetzko, M.F. Peintinger, T. Bredow, Implementation of empirical dispersion corrections to density functional theory for periodic systems, J. Comput. Chem. 33 (2012) 2023–2031.
[20] Y.u. Takano, K.N. Houk, Benchmarking the conductor-like polarizable continuum model (CPCM) for aqueous solvation free energies of neutral and ionic organic molecules, J. Chem. Theory Comput. 1 (1) (2005) 70–77.
[21] Z. Vajglová, N. Kumar, M. Peurla, J. Peltonen, I. Heinmaa, D.Y. Murzin, Synthesis and physicochemical characterization of beta zeolite–bentonite composite materials for shaped catalysts, Catal. Sci. Technol. 8 (23) (2018) 6150–6162.
[22] R. Suerz, K. Eränen, N. Kumar, J. Wärnå, V. Russo, M. Peurla, A. Aho, D. Yu. Murzin, T. Salmi, Application of microreactor technology to dehydration of bio-ethanol, Chem. Eng. Sci. 229 (2021) 116030, https://doi.org/10.1016/j.ces.2020.116030.
[23] D.Y. Murzin, B. Kusema, E.V. Murzina, A. Aho, A. Tokarev, A.S. Boymirzaev, J. Wärnå, P.Y. Dapsens, C. Mondelli, J. Pérez-Ramírez, T. Salmi, Hemicellulose arabinogalactan hydrolytic hydrogenation over Ru-modified H-USY zeolites, J. Catal. 330 (2015) 93–105.
[24] A. Aho, N. Kumar, K. Eränen, T. Salmi, M. Hupa, D.Y. Murzin, Catalytic pyrolysis of biomass in a fluidized bed reactor: influence of the acidity of H-beta zeolite, Process Saf. Environ. Prot. 85 (5) (2007) 473–480.
[25] P. Mäki-Arvela, N. Kumar, V. Nieminen, R. Sjöholm, T. Salmi, D.Y. Murzin, Cyclization of citronellal over zeolites and mesoporous materials for production of isopulegol, J. Catal. 225 (1) (2004) 155–169.
[26] N. Kumar, M. Tiitta, T. Salmi, H. Österholm, WO 2006/070073A1, 2006.
[27] R.G. Pearson, Recent advances in the concept of hard and soft acids and bases, J. Chem. Educ. 64 (7) (1987) 561, https://doi.org/10.1021/ed064p561.
[28] M. Laluc, P. Mäki-Arvela, A.F. Peixoto, N. Li-Zhulanov, T. Sandberg, N.F. Salakhutdinov, K. Volcho, C. Freire, A.Y. Sidorenko, D.Y. Murzin, Catalytic synthesis of bioactive 2 H-chromene alcohols from (−)-isopulegol and acetone on sulfonated clays, React. Kinet., Mech. Catal. 129 (2) (2020) 627–644.